https://doi.org/10.2352/ISSN.2470-1173.2020.10.IPAS-135

Computational Color Constancy under Multiple Light Sources

Jaeduk Han, Soonyoung Hong, and Moon Gi Kang; School of Electrical and Electronic Engineering, Yonsei University, 50 Yonsei-ro, Seodaemun-gu, Seoul 03722, Republic of Korea

Abstract

Without sunlight, imaging devices typically depend on various artificial light sources. However, scenes captured with the artificial light sources often violate the assumptions employed in color constancy algorithms. These violations of the scenes, such as non-uniformity or multiple light sources, could disturb the computer vision algorithms. In this paper, complex illumination of multiple artificial light sources is decomposed into each illumination by considering the sensor responses and the spectrum of the artificial light sources, and the fundamental color constancy algorithms (e.g., gray-world, gray-edge, etc.) are improved by employing the estimated illumination energy. The proposed method effectively improves the conventional methods, and the results of the proposed algorithms are demonstrated using the images captured under laboratory settings for measuring the accuracy of the color representation.

Introduction

Demand of digital imaging devices is rapidly increasing, and various imaging systems have been utilized for many purposes. Recently, computer vision algorithms are applied to many fields, such as object recognition and tracking, image retrieval, or feature extraction. The digital camera, the eye of the vision algorithms, basically depends on light sources for capturing the scene. Especially at night, various artificial light sources have been employed as active illumination sources for the imaging device. However, real world images have huge variations of the illumination conditions. Human vision has the tendency to correct for the effects of the illumination color, but the digital cameras do not have a mechanism to estimate the illumination source [1]. The ability to account for the color of the light source is called color constancy [2].

Most of the digital images are generated by the combination of illumination sources and the reflection or absorption of the energy from objects in the scene being imaged. The light energy captured by the imaging sensor is usually represented as below:

$$\mathbf{f}_{\mathrm{x}} = \begin{bmatrix} f_R \\ f_G \\ f_B \end{bmatrix} = \int_v s(\lambda) I(\lambda) L(\mathrm{x},\lambda) d\lambda, \tag{1}$$

where $\mathbf{f}_{\mathrm{x}}$ is often called pixel values with the coordinate x, f_R, f_G, and f_B denote the color channels of a single pixel, $s = [s_R\ s_G\ s_B]^{\mathrm{T}}$ denotes the spectral sensitivity functions of the imaging device, $I(\lambda)$ indicates the illumination or the energy of light sources, $L(\mathrm{x},\lambda)$ indicates the reflectance of the scene, and v is the visible band. In the literature, the illumination is regarded as a function with respect to the wavelength λ, but in real world images, the illumination should be considered as the function with respect to both coordinate x and wavelength λ. Therefore, the illumination condition should be modeled based on the spatially variant system so the illumination should be rewritten as $I(\mathrm{x},\lambda)$.

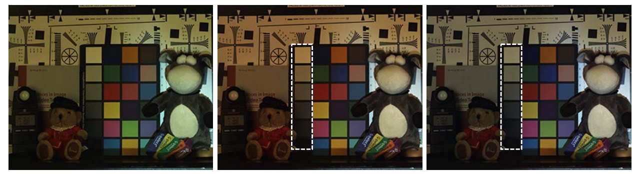

(a) (b) (c)

Figure 1. *Problem of the complex illumination. (a) Test image captured based on the laboratory setting under two different illumination sources. 5500K fluorescent and 6500K LED lighting were used; (b) Output of the gray-edge algorithm [4]. The colors of the color checker were not inappropriately estimated; (c) Output of the proposed color constancy algorithm. The gray-edge algorithm was improved by adopting the proposed illumination estimation algorithm.*

For the accurate observation of colors, the color stimulus, which is clearly the product of the reflectance and the illumination, should incorporate the spatially variant illumination [3]. In general, estimating the illumination of a single image is considered an ill-posed problem, and by considering the spatially varying illumination, the problem becomes more complicated. Nevertheless, the spatially varying function $I(\mathrm{x},\lambda)$ should be adopted for increasing the performance of the computational color constancy algorithms. Figure 1 demonstrates the problem will be covered. The scenes obtained under spatially variant illumination conditions will be analyzed based on (1), which is called the Lambertian model. Note that in Figure 1 (b), without adopting the spatially varying functional for the illumination, the neutral patches marked by the white rectangles in the color checkers look reddish after the color constancy algorithm [4].

The non-uniform distribution of the illumination energy and the multiple light sources with various color temperatures cannot be incorporated by the computational color constancy algorithms, such as gray-world [5], max-RGB [6], shade of gray [7], and gray-edge [4]. Most of the color constancy algorithms adopt the simple Lambertian model of (1), and their assumptions about the spatially invariant illumination (i.e., uniform illumination condition) should be modified for accommodating the illumination conditions of multiple light sources. The pixel value with the Lambertian model considering the spatially varying illumination conditions can be represented as follows,

$$\mathbf{f}_{\mathrm{x}} = \int_v s(\lambda) I(\mathrm{x},\lambda) L(\mathrm{x},\lambda) d\lambda, \tag{2}$$

where $I(\mathrm{x},\lambda)$ indicates the illumination condition with multiple light sources. Based on the linearity of the light energy (which is demonstrated in Figure 2, the spatially varying illumination could be regarded as a linear sum of each light energy from the illuminants, i.e., $I(\mathrm{x},\lambda) = \sum_t I_t(\mathrm{x},\lambda)$, and t denotes the artificial light source, such as LED lighting.

In this paper, the spectral sensitivity functions of each band (R,G,B) are employed to estimate the illumination to solve the problems of spatially varying illumination. Provided the spectrums of light sources are available as prior information, the response of imaging sensors to the artificial illumination would be predictable.

Related Work

The proposed method analyzes illumination conditions of the multiple light sources using the characteristic of a charge-coupled device (CCD). Each artificial light source could be specified by the response to the CCD, which has its own spectral sensitivity function. Therefore, to implement the proposed method, the sensor's responses to the light sources should be investigated beforehand.

Sensor response to the artificial light source

The observed illumination of a single image usually obtained by low-pass filtering [8], because spatial smoothness is assumed in the filed of the illumination. We also estimate the illumination components by convolving the observed image with the Gaussian blur kernel. The energy of the artificial light source α, obtained after the low-pass filtering, can be written as below:

$$\mathbf{e}_{(\alpha,\mathrm{x})} = \begin{bmatrix} e_{\alpha,R} \\ e_{\alpha,G} \\ e_{\alpha,B} \end{bmatrix} = \int_v s(\lambda) I_\alpha(\mathrm{x},\lambda) d\lambda, \tag{3}$$

where $\mathbf{e}_{(\alpha,\mathrm{x})}$ indicates the color of the light source α (note that α denotes the artificial illuminants such as LED, fluorescent, or incandescent lighting.).

The spectrum of the widely used artificial light sources can be measured by spectrometers. The CCD could be also used to evaluate the characteristic of the artificial light sources by utilizing the spectral sensitivity functions $s(\lambda)$. Figure 2 demonstrates that the linearity of the sensor and that the sensor response to the certain light source is fixed even under the condition in which multiple light sources are simultaneously employed. The experiment of Figure 2 shows that each artificial light source possesses its own spectral response. The CCD, which counts the photons, linearly measures the energy of R, G, and B bands, and the energy could be approximated as below:

$$\mathbf{e}_{(\alpha,\mathrm{x})} \approx e_\alpha(\mathrm{x}) \begin{bmatrix} \mu_{(\alpha,R)} \\ \mu_{(\alpha,G)} \\ \mu_{(\alpha,B)} \end{bmatrix} = e_\alpha(\mathrm{x}) \mu_\alpha, \tag{4}$$

where μ_α is a response ratio of each band denoting the captured energy filtered by s, and $e_\alpha(\mathrm{x})$ is the total amount of energy from the light source α in the visible band, i.e.,

$$e_\alpha(\mathrm{x}) = \int_v I_\alpha(\mathrm{x},\lambda) d\lambda. \tag{5}$$

The energy of a single light source α, i.e., $e_\alpha(\mathrm{x})$, is a function with respect to x for modeling the spatially variant illumination and means the energy captured on a single pixel of x.

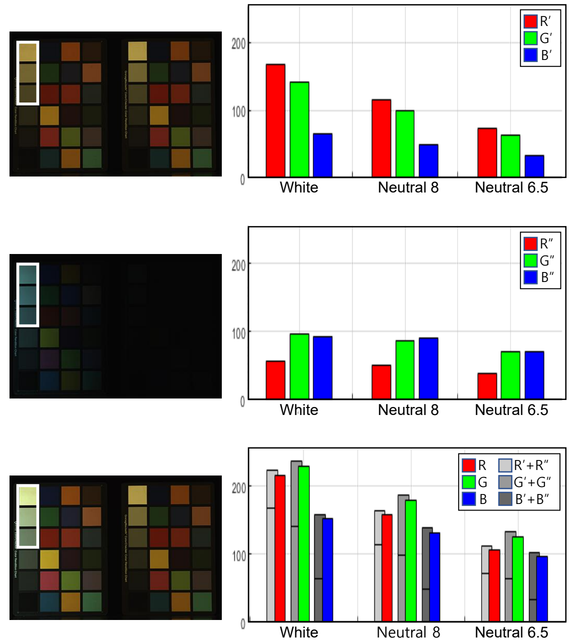

Figure 2. Color checker under LED lighting. Top: Color checker under 3100K. 3100K LEDs are perceived as yellowish white; Mid: Color checker under 6500K. 6500K LEDs are perceived as bluish white; Bottom: Color checker under 3100K and 6500K. This illumination condition employs the above light sources at the same time. The color patches in the white rectangles are visualized. The measured pixel values (R, G, B) under the multiple light sources could be approximated as the sum of the values (R′+R″, G′+G″, B′+B″) under the independent light source. In the case of chromatic patches, similar tendencies are observed.

Our experiments were conducted under light sources denoted by the color temperature as 3100K, 5500K, and 6500K. We used two types of light sources, LED of 3100K and 6500K and fluorescent bulb of 5500K. Each artificial light sources lit the color checker in the darkroom. The response ratio μs ($|\mu| = 1$) are measured on the achromatic patch as in Figure 2. The response ratio μs, which are the spectral characteristics of light sources, are obtained in our experiments as below:

$$\begin{aligned} \mu_{3100K} &= [0.442, 0.380, 0.178]^{\mathrm{T}}, \\ \mu_{5500K} &= [0.363, 0.426, 0.211]^{\mathrm{T}}, \\ \mu_{6500K} &= [0.235, 0.396, 0.369]^{\mathrm{T}}. \end{aligned} \tag{6}$$

The set of μs are used as a dictionary in our method. Various information about the artificial illuminations enables our method to estimate the illumination condition precisely.

Proposed method

Our derivation for the illumination estimation departs from the illumination condition of two light sources denoted by α and β, respectively. Note that the proposed method can estimate the illumination with up to three light sources because typical imaging devices use the Bayer color filter array employing three bands [9]. Our methods can be extended by accommodating the wide band which contains invisible light waves (e.g., infrared) or by employing other color filter arrays (e.g., RGBW color filter array).

Figure 3. Visualized solution of (9). The images in the top row are the decomposed illumination, and the images in the bottom row are the captured under the single artificial light source independently for comparison.

Illumination estimation

The illumination $I(\mathrm{x},\lambda)$ can be substituted for the sum of the artificial illuminantion to incorporate the multiple light sources as mentioned in the previous section. The triplets for the illumination color under two light sources, (I_α and I_β) can be represented as below:

$$\mathbf{e}_{\mathrm{x}} = \begin{bmatrix} e_R \\ e_G \\ e_B \end{bmatrix} = \int_v s(\lambda)(I_\alpha(\mathrm{x},\lambda) + I_\beta(\mathrm{x},\lambda))d\lambda. \tag{7}$$

The distributive property of the integral can be applied right-hand side of (7) to accommodate the characteristics of the CCD. The observed illumination color can be rewritten utilizing (3) and (4) as below:

$$\mathbf{e}_{\mathrm{x}} \approx e_\alpha(\mathrm{x})\mu_\alpha + e_\beta(\mathrm{x})\mu_\beta, \tag{8}$$

where μ_α and μ_β are from the set of response ratios.

The observed illumination color is represented as a linear combination of the artificial light sources with prior information μ_α and μ_β, and (8) can be converted into the matrix form, i.e.,

$$\mathbf{e}_{\mathrm{x}} \approx [\mu_\alpha|\mu_\beta] \begin{bmatrix} e_\alpha(\mathrm{x}) \\ e_\beta(\mathrm{x}) \end{bmatrix} = \mathrm{M}\hat{\mathbf{e}}_{\mathrm{x}}, \tag{9}$$

where $\hat{\mathbf{e}}_{\mathrm{x}}$ denotes the artificial illumination to be estimated. The matrix M can be inversed by various methods such as the least squares approximation. The images of the top row in Figure 3 demonstrate the visualized solution of (9) which can be obtained as below:

$$\hat{\mathbf{e}}_{\mathrm{x}} = \mathrm{M}^\dagger \mathbf{e}_{\mathrm{x}}, \tag{10}$$

where $\mathrm{M}^\dagger$ denotes the inverse matrix of M. The solution of (9) is the estimated energy of each light source. Light from the multiple illuminants is decomposed by (10) in which the components of $\hat{\mathbf{e}}_{\mathrm{x}}$ mean the decomposed light energy captured in a single pixel.

Improving color constancy algorithms

The conventional methods could be improved by utilizing the decomposed illumination $\hat{\mathbf{e}}_{\mathrm{x}}$. To estimate the spatially variant illumiation, the input image is decomposed into two signals. The decomposed signal $\mathbf{f}^\alpha$, which is the region affected by the illuminant α, is obtained as follows:

$$\mathbf{f}^\alpha = \mathbf{f} \otimes \frac{\mathbf{e}_\alpha}{(\mathbf{e}_\alpha + \mathbf{e}_\beta)}, \tag{11}$$

where $\mathbf{f}$ is the input image, $\otimes$ is the componentwise product, and $\mathbf{e}_\alpha$ the signal consists of $e_\alpha(\mathrm{x})$. The decomposed signal of the illuminant β is obtained in the same manner. To estimate the illumination condition, $\mathbf{f}^\alpha$ and $\mathbf{f}^\beta$, which are regarded as decomposed layers, act as an input of the color constancy algorithm independently.

By employing the decomposed signal of (11) as input signals, the assumptions of the static methods of the conventional color constancy algorithms can incorporate the spatially varying illumination conditions. The assumption of the edge-based algorithm [4] with our estimation method is represented as follows:

$$\frac{\int \left|\partial^n L_\zeta(\mathbf{x},\lambda)\right| dx}{\int \mathbf{x}^n} = g(\lambda) = k, \tag{12}$$

where L_ζ denotes the reflectance components affected by the single illumination and $\zeta \in \{\alpha,\beta\}$. Similarly, assumptions of other conventional methods can solve the problems due to the complex illumination conditions by employing the decomposed signals.

Experimental Results

Computational color constancy algorithms

Differences in illumination cause the imaging devices to measure object colors to be biased toward the color of the light source [10]. The color constancy algorithms, separated in three groups: static, gamut-based, and learning-based methods, correct for the effects of the color of light [1]. In this paper, the static methods are improved by considering the sensor response mentioned in the previous section. The static methods are simpler and faster than other groups, but vulnerable to the illumination conditions with non-uniform multiple light sources as demonstrated in Figure 1.

The static methods are explained by a single framework incorporating the gray-world and gray-edge hypotheses [4]. The framework is written as below:

$$\left(\int \left|\frac{\partial^n \mathbf{f}_\sigma(\mathbf{x})}{\partial \mathbf{x}^n}\right|^p\right)^{1/p} = k\mathbf{e}^{n,p,\sigma}, \tag{13}$$

where $\mathbf{f}_\sigma = \mathbf{f} * G_\sigma$ is the convolution of an input image with a Gaussian filter with a parameter σ, p is the Minkowski-norm (for detail, refer to [1, 4, 10]). Various algorithms are represented by the symbol (n,p,σ), and gray-world [5] with (0,1,0), max-RGB [6] with (0,∞,0), shade of gray [7] with (0,7,0), and gray-edge [4] with (1,7,4) are improved. The improved algorithms are represented based on (13) as bellow:

$$\left(\int \left|\frac{\partial \mathbf{f}^\alpha_\sigma(\mathbf{x})}{\partial \mathbf{x}^n}\right|^p\right)^{1/p} + \left(\int \left|\frac{\partial \mathbf{f}^\beta_\sigma(\mathbf{x})}{\partial \mathbf{x}^n}\right|^p\right)^{1/p} = k\mathbf{e}^{n,p,\sigma}_\alpha + l\mathbf{e}^{n,p,\sigma}_\beta, \tag{14}$$

where $\mathbf{e}_\alpha$ and $\mathbf{e}_\beta$ are colors of the artificial light sources.

Measurements

Several experiments were conducted to measure the performance of the improved algorithm, in comparison with the corresponding original algorithm. Figure 4 shows the final results. The algorithms adopting the proposed illumination estimation show more accurate values on the color checker in terms of the angular error. The images used in our experiments contain the color

(a) (b) (c) (d) (e)

Figure 4. *Experimental results of various algorithms. (a) Top: input image illuminated by multiple light sources, 6500K (left-hand side) and 5500K (right-hand side). Bottom: results of the illumination decomposition; (b) Top: gray-world. Bottom: improved gray-world; (c) Top: max-RGB. Bottom: improved max-RGB; (d) Top: shade of gray. Bottom: improved shade of gray; (e) Top: gray-edge. Bottom: improved gray edge.*

checker, and the achromatic patches were utilized to evaluate the performance. For the objective assessment, the angular error is represented as below:

$$\text{angular error} = \cos^{-1}(\widetilde{\mathbf{v}}_o \cdot \widetilde{\mathbf{v}}_r), \tag{15}$$

where $\widetilde{\mathbf{v}}_o$ is a normalized vector derived from the observed achromatic patches, and $\widetilde{\mathbf{v}}_r$ a normalized reference vector. Table 1 demonstrates the angular errors measured based on the obtained results. In most cases, the improved versions recorded lower values which mean more accurate estimation.

Table 1: Measured angular errors form the test images. The proposed algorithms are marked with (i) which means improved by the proposed illumination estimation method.

	image1	image2	image3
Input	18.9	15.7	13.3
Gray world [5]	11.8	**8.6**	6.7
Gray world(i)	**11.6**	8.8	**6.5**
Max-RGB [6]	24.4	17.6	**7.8**
Max-RGB(i)	**18.2**	**11.3**	9.8
SoG [7]	18.0	17.6	10.3
SoG(i)	**10.6**	**14.0**	**9.2**
Gray edge [4]	22.2	21.4	9.7
Gray edge(i)	**10.4**	**17.3**	**8.9**

Conclusion

The illumination estimation method to improve the computational color constancy algorithms is proposed utilizing the sensor response to the artificial illumination. Based on the prior information, the conventional methods with the low complexity are improved. The improvement scheme can be applied to not only the color constancy but also other algorithms (e.g., contrast enhancement or auto focusing algorithm) that are suffering from the aforementioned illumination conditions.

Acknowledgment

This work was supported by the National Research Foundation of Korea(NRF) grant funded by the Korea government(MSIT) (No. 2019R1A2C2002167).

This research was partially supported by the Graduate School of YONSEI University Research Scholarship Grants in 2018.

References

[1] A. Gijsenij, T. Gevers and J. van de Weijer, ”Computational Color Constancy: Survey and Experiments,” in IEEE Transactions on Image Processing, 20, 9, 2011, pg. 2475-2489.

[2] D. A. Forsyth, “A novel algorithm for color constancy,” International Journal of Computer Vision, 5, 1, 1990, pg. 5–35.

[3] Edwin H. Land and John J. McCann, “Lightness and retinex theory,” J. Opt. Soc. Am., 61, 1, 1971, pg. 1–11.

[4] J. van de Weijer, T. Gevers, and A. Gijsenij, “Edge-based color constancy,” IEEE Transactions on Image Processing, 16, 9, 2007, pg. 2207–2214.

[5] G. Buchsbaum, “A spatial processor model for object colour perception,” Journal of the Franklin Institute, 310, 1, 1980, pg. 1 – 26.

[6] Edwin H. Land, “The retinex theory of color vision,” Scientific American, 237, 6, 1977, pg. 108–129.

[7] Graham D. Finlayson and Elisabetta Trezzi, “Shades of gray and colour constancy,” Color and Imaging Conference, 2004, 1, 2004.

[8] Moon Gi Kang Ki Sun Song, Hee Kang, “Contrast enhancement algorithm considering surrounding information by illumination image,” Journal of Electronic Imaging, 23, 2014, pg. 23 – 23 – 18.

[9] B. Bayer, “Color imaging array,” US Patent 3 971 065, 1976.

[10] A. Gijsenij and T. Gevers, “Color constancy using natural image statistics and scene semantics,” IEEE Transactions on Pattern Analysis and Machine Intelligence, 33, 4, 2011, pg. 687–698.

Author Biography

Jaeduk Han received his BS. degree in electronics engineering in 2014 from Yonsei University, Seoul, Korea. He is currently pursuing a Ph.D. at the Department of Electrical and Electronic Engineering at Yonsei University. His current research interests include the inverse problems in image and video processing.

Soonyoung Hong received the B.S. degree in electrical and electronic engineering from Yonsei University, Republic of Korea, in 2015. Currently, he is pursuing the joint M.S. and Ph.D. degree with the Department of Electrical and Electronic Engineering at Yonsei University. His current research interests are contrast enhancement and high dynamic range.

Moon Gi Kang received Ph.D. degree in electrical engineering from Northwestern University, USA in 1994. He is currently a professor at the Department of Electronic Engineering of Yonsei University, Korea. He has served as the Editor of SPIE Milestone Series Volume (CCD and CMOS imagers), the Guest Editor of the IEEE SP Magazine Special Issue on Superresolution Image Reconstruction (May 2003), the Associate Editors of the EURASIP Journal of ASP and the Elsevier Journal of Digital Signal Processing.